Braiding two polymer chains into a double helix with a molecular rotor

Maxime Ledent,[1] Damien Sluysmans,[1] Philippe Schiel,[2] Damien Dattler,[2] Quan Li,[2] Thomas Ellis,[2] Nicolas Giuseppone,[2,3]* Anne-Sophie Duwez[1]*

[1] UR Molecular Systems, Department of Chemistry, University of Liège, Liège, Belgium

[2] SAMS Research Group, Université de Strasbourg, CNRS, Institut Charles Sadron UPR 22, Strasbourg, France.

[3] Institut Universitaire de France (IUF), Paris, France.

* Correspondence and requests for materials should be addressed to A.-S.D. (asduwez@uliege.be, force spectroscopy experiments) or N.G. (giuseppone@unistra.fr, synthesis)

Abstract

The control of molecular motion to produce well-defined mechanical effects or tasks remains inherently challenging due to random Brownian motion. Although directional motion at the molecular scale has been widely demonstrated, its translation into controlled molecular architectures remains limited. Here, we show that a rotary molecular motor can actively direct the assembly of two polymer chains into a double-helical structure. Two poly(ethylene oxide) chains were covalently anchored to an overcrowded alkene-based motor, whose unidirectional rotation is driven by UV-light. The resulting motor-induced entanglement was probed by single-molecule force spectroscopy, revealing distinct mechanical signatures, including force plateaus and twist–stretch coupling behaviour, consistent with the formation of intertwined polymer chains in a double-helical arrangement reminiscent of DNA. These findings demonstrate how molecular rotary motion can be harnessed to induce controlled long-range mechanical organization, enabling the propagation of nanoscale motion into well-defined supramolecular assemblies and establishing design principles for motor-driven molecular architectures.

Introduction

The remarkable functionality and controlled motion exhibited by biological molecular machines have long inspired the development of artificial, stimuli-responsive molecular motors[1]. Motivated by natural rotary systems such as adenosine triphosphate synthase[2,3], chemists have sought to design synthetic analogues capable of achieving controlled unidirectional rotation. This objective was first realized by Feringa and co-workers in 1999 with the development of a light-driven motor based on double-bond isomerization in an overcrowded alkene[4]. These motors convert ultraviolet (UV)-light and thermal energy into controlled, unidirectional rotation.

More recently, such mechanically productive motion has been shown to drive the winding of polymer chains in looped figure of eight conformations or in gel networks, leading to the formation of thermodynamically disfavoured entanglements.[5–7] In these systems, star-shaped polymer–motor conjugates act as mechanically active reticulation nodes, enabling out-of-equilibrium actuation. Upon continuous UV irradiation, the embedded motors undergo sustained unidirectional rotation, progressively twisting the covalently attached polymer chains.[5] In gels, the resulting accumulation of torsional strain across the network gives rise to a collective mechanical response, ultimately leading to a macroscopic contraction of the material. Despite these advances, however, experimental examples in which molecular motors drive well-defined mechanical processes with clearly detectable effects remain scarce.

Here, we sought to determine whether the rotation of a single, isolated molecular motor could induce the twisting of a pair of polymer chains directly attached to its rotor part. To directly probe the mechanical consequences of this rotation at the molecular level, we turned to atomic force microscopy (AFM)–based single-molecule force spectroscopy (SMFS), a powerful technique that provides access to the force–extension response of individual polymer systems. SMFS has been extensively used to investigate the mechanical properties of polymers,[8] supramolecular assemblies,[9] and biomacromolecules,[10] and has more recently emerged as a valuable tool to study the operation and work generation of synthetic molecular machines and motors.[11–15] In particular, SMFS enables the identification of distinct molecular conformations through their characteristic mechanical signatures, allowing one to distinguish between random coils, entangled structures, and ordered assemblies. Previous studies have demonstrated its ability to capture mechanically induced transitions such as helix–coil transformations[16–18] and the unwinding of DNA-like structures.[19,20] Within this framework, we hypothesized that motor-induced entanglement or helical organization of polymer chains would generate specific and detectable features in the force–distance profiles.

Accordingly, we employed SMFS to probe the response of individual polymer–motor conjugates under UV irradiation, with the aim of establishing a direct link between molecular rotary motion and the emergence of controlled polymer architectures.

Results and discussion

Sample preparation prior to AFM experiments.

To enable single-molecule force spectroscopy measurements, we designed polymer–motor systems that could be robustly anchored to a surface while maintaining sufficient spatial isolation between individual conjugates. Bis-alkyne bis-PEG_{5000} light-driven rotary motor **1** (Figure 1a) and its non-rotary episulfide analog **2** (Figure 1b) were synthesized and fully characterized (see detailed protocols in Supporting Information sections 1 and 2). To prepare for motor grafting, plasma activated silicon wafers were first functionalized by silanization with aliphatic azides, providing a reactive platform for subsequent coupling. The motor and a passivating alkyne (1-decyne) were then co-grafted onto the surface via a copper-catalyzed Huisgen [3+2] cycloaddition ("click" reaction). Importantly, the ratio between motor and passivator was carefully tuned to achieve a low surface density of approximately 0.25 motor.nm^{-2}. This dilution strategy ensures that individual polymer–motor conjugates can be selectively addressed during AFM-based force spectroscopy measurements (see detailed protocols in Supporting Information, Section 3).

SMFS measurements on the polymer–motor conjugates before irradiation

Following grafting, SMFS experiments were performed on the polymer–motor conjugates in the dark to establish the characteristic force–distance profiles of the system prior to irradiation. Approach–retraction cycles of the AFM tip were carried out in *N,N*-dimethylformamide (DMF) at a velocity of 200 nm s^{-1}, enabling the capture and stretching of polyethylene oxide (PEO) chains attached to the rotor (Figure 1c). As the tip–surface separation increases, the restoring force exerted by the polymer rises, yielding characteristic and reproducible force–distance profiles (Figure 2a). The rupture distances correspond to extension values that are in good agreement with the contour length of the polymer–motor conjugate (Figure S1).

We used the worm-like-chain (WLC)[21] model, a statistical mechanical framework describing the entropic elasticity of a flexible polymer in a random coil conformation upon extension, to quantitatively analyze the force profiles. From these fits (Figure 2a, dotted lines), we extracted two key parameters: the contour length (L_c) and the persistence length (l_p). L_c corresponds to the maximum extension of a polymer chain in an entropic regime (*i.e.* without deformation of bond lengths and angles), and is normalized to unity in Figure 2a. l_p represents the smallest segment

pointing in a defined direction and reflets the flexibility of the chain. It governs the initial curvature of the force–distance curves: the lower the l_p, the more flexible the chain.

A gaussian deconvolution of the l_p distribution reveals the presence of two distinct populations centred at 0.18 ± 0.01 and 0.35 ± 0.01 nm (Figure 2b). The second value is in good agreement with reported persistence lengths for a single PEO chain (0.35–0.40 nm),[22] indicating that these events correspond to the stretching of individual polymer chains. By contrast, the most probable value at 0.18 ± 0.01 nm, which is approximately half of the expected value, points to an apparent increase in flexibility of the system. This observation can be rationalized by considering that the persistence length has been shown to scale inversely with the number of polymer chains stretched in parallel.[23–25] In such a situation, the effective flexibility of the system increases due to the additional degrees of freedom introduced by the presence of multiple chains, leading to a reduction in the apparent l_p value. Based on this relationship, we can therefore infer that, during the pulling experiments, two PEO chains are frequently stretched simultaneously (as illustrated in Figure 1c), effectively reducing the measured persistence length by a factor of two. It is thus possible to distinguish when one or two chains have been grabbed by the tip. The relatively high probability of capturing two chains at once can be attributed to the random-coil conformation of PEO in solution. This conformation enhances the likelihood that both chains come into contact with and physisorb onto the AFM tip during the approach–retraction cycle, rather than a single chain being isolated.

SMFS measurements on polymer–motor conjugates after irradiation

Prior to the SMFS experiments, the surfaces were irradiated under UV-light for 1 minute (1.29 W, 0.43 mW cm^{-2} at 366 nm) to trigger the rotation of the molecular motors.[26] Standard SMFS measurements were then performed under the same conditions as described above, ensuring direct comparability with the non-irradiated system. In contrast to the force–distance profiles obtained in the dark, two distinctive features emerged after irradiation: extended plateaus and characteristic S-shaped curves. Importantly, these signatures were systematically observed only after UV activation, indicating that they originate from specific polymer conformations generated by the light-driven unidirectional rotation of the molecular motors. This clear difference highlights the direct impact of motor actuation on the organization of the polymer chains at the single-molecule level.

When sufficiently high forces are reached, a force plateau emerges in the force–distance curves (Figure 3a). Initially, the force increases with extension following a WLC behaviour, characteristic of the stretching of a flexible polymer in a random-coil conformation. The persistence length (l_p)

extracted from this initial regime is approximately 0.37 nm (Figure S2), which is consistent with the stretching of a single PEO chain. Beyond this regime, the force reaches a constant value over a defined extension, forming a plateau. Such behaviour indicates the progressive release of hidden length during elongation and is characteristic of a structural transition, which can be associated with a helix–coil transformation. This interpretation is supported by previous force spectroscopy studies reporting similar plateaus during the unwinding of supramolecular helices[16–18,27] or the melting of double-stranded DNA.[28] After this plateau, the force increases again following a WLC behaviour, until the final rupture event corresponding to the detachment of the molecule from the AFM tip. Notably, comparable plateaus are observed in DNA when only one strand is captured by the AFM tip, leading to the mechanical unwinding of the double helix. In the present case, the observation of a well-defined plateau, combined with the persistence length measured prior to the plateau, strongly suggests that only one PEO chain is directly pulled, while the second chain remains entangled and is progressively released during stretching. We therefore suggest that the unidirectional rotation of the motor under UV irradiation induces the formation of an ordered, double-helical arrangement of the two PEO chains. Under these conditions, the applied force promotes the progressive disentanglement of the chains and induces characteristic mechanical signatures, as described below.

During SMFS experiments, when the tension applied to the pulled PEO chain —entangled with the second one— reaches a threshold of approximately 50 pN, the system begins to disentangle. The plateau can thus be attributed to the progressive release of chain segments initially trapped within the entanglement. At the molecular level, PEO chains arranged in a helical conformation adopt a *trans–trans–gauche* (*ttg*) conformation.[29] Upon stretching, a mechanically induced transition toward a more extended *trans–trans–trans* (*ttt*) conformation occurs, resulting in an increase in contour length that manifests as the observed plateau. The measured plateau force threshold (49 pN, Figure 3b) is in excellent agreement with reported values for the *ttg*-to-*ttt* transition in PEO (~50 pN).[29] Based on an estimated extension of 0.8 Å per monomer unit (corresponding to segment lengths of 2.78 Å and 3.58 Å for *ttg* and *ttt* conformations, respectively), the average plateau length of approximately 2 nm (Figure 3c) corresponds to the isomerization of about 21 monomer units. This represents roughly 20% of the polymer chain being involved in the entangled region. Furthermore, as the torsional strain introduced by successive motor rotations accumulates, the increasing mechanical tension is expected to reduce the quantum yield of the motor, eventually leading to a complete arrest of rotation.[7] In this context, the extent of entanglement observed here already represents a significant fraction of the chain. Insights from crystallographic studies indicate that approximately seven monomer units are

required to complete two helical turns.[30] On this basis, we estimate that the entangled region corresponds to an average of six helical turns, with up to 18 turns for the longest plateau events. By correlating these structural parameters with the number of unidirectional rotations occurring during one minute of UV irradiation, we estimate an average rotation frequency of ~0.1 Hz for this motor, reaching up to ~0.3 Hz when considering the longest plateau events. These values should be regarded as lower-bound estimates of the rotation frequency. Indeed, partial relaxation or disentanglement of the polymer chains between the irradiation period and the force spectroscopy measurement would lead to an underestimation of the actual number of turns generated during motor operation. However, no decrease in plateau length is observed over time, suggesting that the entangled structures remain largely stable once formed and that relaxation processes are limited on the timescale of the experiments. In addition, the accumulation of mechanical strain during the entanglement process may transiently oppose rotation, further increasing the number of motor cycles required to generate a given helical structure. Notably, the estimated rotation frequencies are consistent with previously reported values (~10^{-2} Hz), measured in more constrained systems such as polymer gels, where the increased mechanical resistance is expected to reduce the motor speed.[5] Overall, this agreement supports the consistency of our mechanical analysis with established motor dynamics.

As a control experiment, similar pulling measurements were performed after UV irradiation on a chemically locked motor, in which the central double bond was replaced by an episulfide moiety[5] (Figure 1b). In this configuration, the cyclic structure —instead of a double bond between the stator and the rotor— prevents access to the excited-state geometry required for isomerization, thereby inhibiting the unidirectional rotation mechanism described above. In striking contrast to the active system, no force plateaus were observed in the corresponding force–distance curves. This absence of plateaus unambiguously demonstrates that the formation of the double-helical arrangement of the PEO chains is a direct consequence of motor operation, rather than a nonspecific effect of UV irradiation or polymer interactions alone.

A second distinctive force–distance profile was identified in the form of S-shaped curves, characterized by an inverted curvature (Figure 4). These signatures are attributed to cases where both polymer chains are simultaneously captured and stretched by the AFM tip. Initially, the response follows a classical WLC behaviour corresponding to the stretching of the polymer–motor conjugate. At higher extensions, however, a clear deviation from this model appears, marked by a reversal in the curvature of the force–distance trace. Such S-shaped features have previously

been reported during the stretching of DNA,[31] where they are attributed to an overwinding of the double helix that leads to an extension of the molecule.[32] This behaviour arises when both strands are engaged during pulling and results from a coupling between torsion and extension, known as twist–stretch coupling.[33] In this regime, the applied mechanical force induces additional twisting of the helix, which in turn modifies its extension, giving rise to a characteristic deviation from the WLC prediction.[32] By analogy, the observation of similar S-shaped signatures in our system strongly supports the formation of an intertwined structure involving two PEO chains. The presence of such twist–stretch coupling behaviour therefore provides further evidence that the motor-driven rotation under UV irradiation generates a double-helical organization of the two PEO chains.

Finally, force–distance profiles consisting of a single rupture peak were also observed. These events arise when the interaction between the PEO chain and the AFM tip is too weak to sustain the forces required for unwinding the helical structure (Figure 3b). As a result, the polymer detaches from the tip before the characteristic plateau or S-shaped signatures can develop. Interestingly, a significant fraction of these single-peak profiles exhibits l_p values exceeding the theoretical value expected for individual PEO chains. To better understand this behaviour, Figure 5a presents the l_p distribution as a function of the rupture distance. A clear correlation emerges, with higher l_p values associated with larger rupture extensions. Such elevated l_p values are indicative of a significantly more rigid system, which can be rationalized by a high degree of entanglement between the PEO chains, leading to the formation of a compact helical structure (Figure 5b).

Assuming that the ethylene oxide units predominantly adopt a *trans–trans–gauche* (*ttg*) conformation within this helical arrangement, the average rupture length of 32 nm, obtained from gaussian deconvolution (Figure 5a, top panel) corresponds to approximately 116 monomers units within the high-l_p structure. This estimate is based on a crystallographic fiber period of 1.925 nm for seven monomer units, corresponding to two helical turns.[30] This value closely matches the total length of the polymer chain (113 monomers), with the slight difference likely reflecting the formation of a double-helical structure rather than a single helix. On this basis, we estimate that up to 32 unidirectional rotation cycles are required to fully braid the polymer chains into these highly rigid configurations. This number suggests that higher effective rotation frequencies (potentially up to ~0.6 Hz) may be reached for the most extended structures, compared to those inferred from the plateau analysis. The relatively broad distribution of l_p values further reflects the presence of structural heterogeneity within the helix, likely arising from occasional *trans–trans–*

trans (*ttt*) defects, which locally affect both the rigidity and the extension of the system. Overall, the correlation between increased persistence lengths and larger rupture distances provides additional evidence for the formation of highly ordered, entangled structures. Consistently, control SMFS experiments performed on the episulfide-based, non-rotating motor, after UV irradiation do not exhibit such elevated l_p values (Figure S3), confirming that this behaviour originates from motor-driven organization of the polymer chains.

Taken together, the emergence of force plateaus, S-shaped profiles, and enhanced persistence lengths provides consistent and complementary evidence that light-driven motor rotation induces the formation of double-helical structures, establishing a direct link between molecular motion and controlled mechanical structuring at the single-molecule level.

Conclusion

In summary, we provide direct experimental evidence of molecular motor-driven braiding of two polymer chains within polymer–motor conjugates, probed at the single-molecule level using AFM-based SMFS. Prior to irradiation, the system exhibits a stochastic random-coil conformation, characterized by classical WLC behaviour. The emergence of a persistence length population at $l_p \approx 0.18$ nm further reveals the ability to distinguish events in which two polymer chains are stretched simultaneously.

Upon UV irradiation, the force–distance response of the polymer–motor conjugates is profoundly altered, reflecting the propagation of the motor's unidirectional rotation through the polymer system. The appearance of force plateaus at 49 pN —consistent with the *ttg*-to-*ttt* isomerization of PEO— and S-shaped signatures characteristic of twist–stretch coupling collectively demonstrate a transition from disordered coils to ordered, double-helical structures arising from motor-driven entanglement. Quantitative analysis of the plateau events indicates that, on average, approximately 20% of the polymer chain becomes trapped within the entangled structure, corresponding to about six unidirectional rotation cycles, before the resulting internal tension limits further rotation. Extending this analysis to the most entangled configurations reveals that up to several tens of rotation cycles can be accumulated, enabling the formation of highly extended double-helical architectures and indicating effective rotation frequencies close to the Hz range. In addition, the correlation between increased persistence lengths and larger rupture distances provides further evidence for the formation of rigid, intertwined supramolecular architectures. Crucially, the absence of such features in chemically locked episulfide controls confirms that the observed organization arises directly from motor activity.

Taken together, these findings establish a clear causal link between sub-nanometre rotary motion and controlled mechanical organization at larger length scales. Importantly, these results show that the motion of a single synthetic molecular motor can be harnessed to drive the formation of double-helical architectures from flexible polymer chains. More broadly, they demonstrate how directional molecular motion can be harnessed to impose order within otherwise disordered polymer systems.[34] This ability to translate nanoscale actuation into programmable mechanical properties represents a key step towards the design of active, out-of-equilibrium materials with tunable stiffness, controlled entanglement, and light-responsive behaviour. Ultimately, mastering the coupling between molecular machines and polymer mechanics opens new avenues for the development of synthetic systems with increasingly complex, functionally integrated dynamics, approaching those of biological machinery.

Supplementary Information

See Supplementary Information for detailed methods and protocols: Details of the synthesis of all molecules, NMR data, details of force spectroscopy experiments and supplementary figures.

Acknowledgments

This work was supported by the European Research Council (ERC Advanced Grant 101054338, to A.-S.D.; and ERC Advanced Grant 101199917 to N.G.), the F.R.S.-FNRS (CDR J.0074.22, GEQ U.G017.22, and EQP U.N032.18 to A.-S.D.), and the Foundation Jean-Marie Lehn (CIRCULAR project fellowship to D.T.).

Author Contributions

A.-S. D., M. L., and N. G. designed the experiments. P. S., D. D., Q. L. and T. E. carried out the chemical synthesis, characterization studies, and grafting onto surfaces. M.L. performed the AFM experiments and M.L. and D.S. analyzed the data. A.-S.D. and N. G. directed the research. M.L. and A.-S. D. wrote the paper. All the authors discussed the results and commented on the manuscript.

Declaration of Interests

The authors declare no competing interests.

Methods

See Supplementary Information for detailed methods and protocols.

Synthesis of molecular motors.

See SI

Grafting onto silica surfaces.

See SI

SMFS experiments.

Single-molecule force spectroscopy experiments were performed using an MFP-3D Origin+ atomic force microscope (Asylum Research, Oxford Instruments) equipped with OBL-10 Biolever cantilevers (Bruker) with a nominal spring constant of k = 0.03 N·m^{-1}. Prior to each experiment, the cantilevers were calibrated in air using both the thermal noise method and the Sader method to ensure accurate force measurements. Approach–retraction cycles were conducted in N,N-dimethylformamide at a constant velocity of 200 nm·s^{-1}, with a sampling rate of 17 kHz. During the approach phase, the AFM tip was brought into contact with the surface until a contact force of 500 pN was reached, ensuring the physisorption of polymer chains onto the cantilever tip.

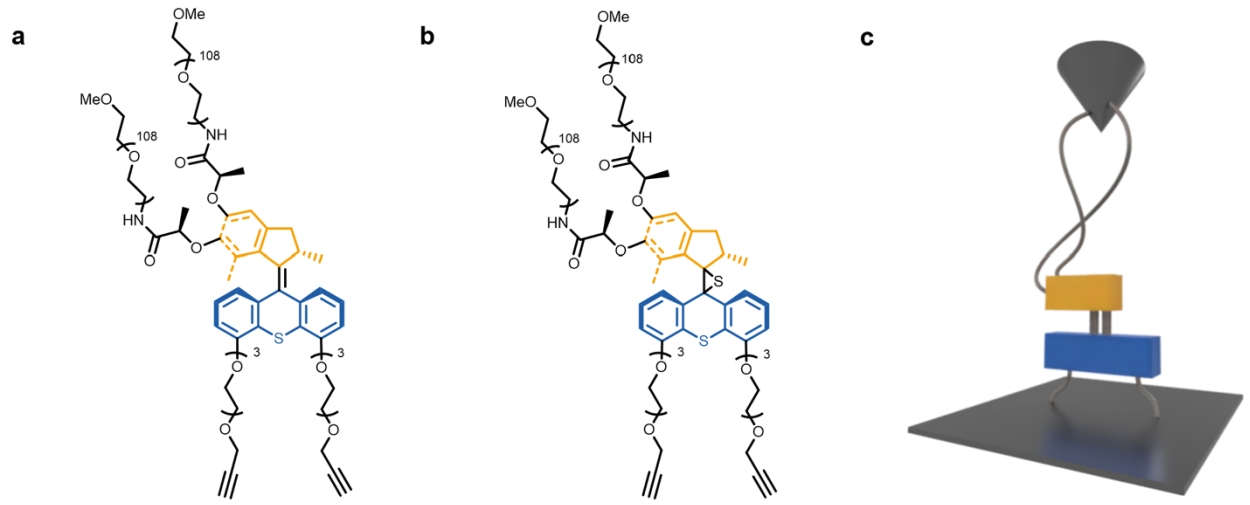

Figure 1. Design of the polymer–motor conjugates and experimental setup. **a.** Chemical structure of the polymer–motor conjugate based on an overcrowded alkene rotary motor. **b.** Chemical structure of the control conjugate incorporating an episulfide cycle, which chemically locks the rotation. **c.** Schematic representation of the SMFS experiment used to probe the mechanical response of individual conjugates.

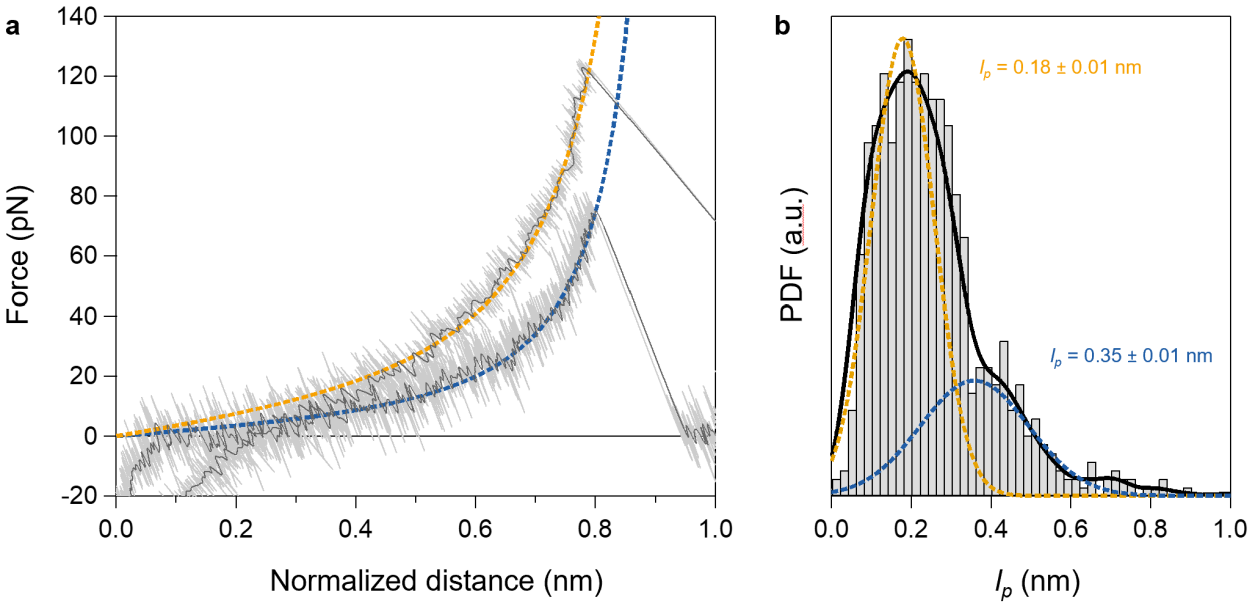

Figure 2. Force–distance analysis of polymer–motor conjugates prior to irradiation. a. Superposition of representative force–distance curves obtained in DMF on the polymer–motor conjugate before UV irradiation. Distances are normalized by their contour length obtained from

WLC fitting. The blue curve corresponds to a l_p value of 0.35 nm, characteristic of the stretching of a single PEO chain, whereas the orange curve (l_p = 0.18 nm) is assigned to the simultaneous stretching of two PEO chains in parallel. **b.** Histogram of the extracted l_p values (N = 638). The black trace represents the probability density function, while the dashed orange and blue lines correspond to gaussian fits associated with the two populations.

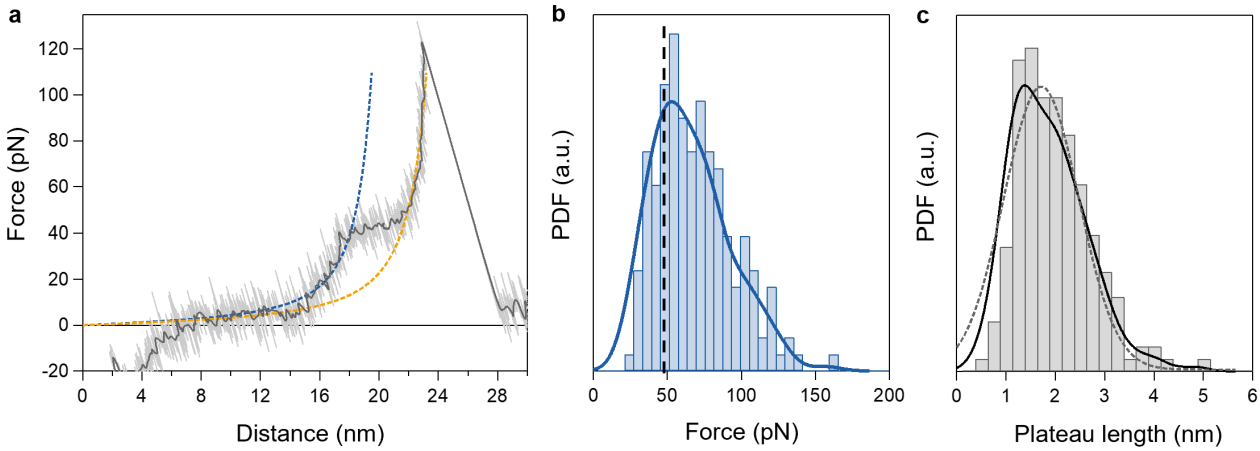

Figure 3. Mechanical signature of motor-induced entanglement after UV irradiation. **a.** Representative force–distance curve displaying a plateau, recorded on a polymer–motor conjugate after UV irradiation. The raw signal is shown in light grey and the smoothed curve in dark grey. WLC fits applied before and after the plateau are shown as blue and orange dashed lines, respectively. **b.** Histogram and corresponding probability density function of the force at the onset of the plateau (49 pN ± 2 pN). The dashed black line indicates the average rupture force associated with detachment of the polymer–motor conjugate from the AFM tip, showing that in most cases the tip–PEO bond breaks before reaching the plateau force. **c.** Histogram of the plateau lengths, together with the probability density function (solid line) and Gaussian fit (dashed line), yielding an average value of 1.7 ± 0.1 nm).

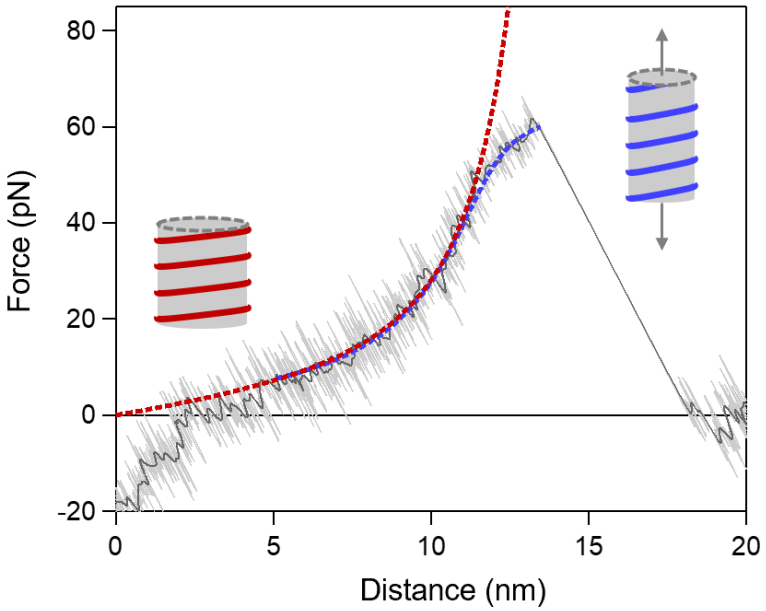

Figure 4. S-shaped force–distance profiles revealing twist–stretch coupling. Representative force–distance curve of a polymer–motor conjugate recorded after UV irradiation. The raw signal is shown in light grey and the smoothed curve in dark grey. At low extensions, the response follows classical WLC behaviour (red fit), characteristic of the elastic stretching of the system. At higher forces, a clear deviation from this model appears, manifested as an inverted curvature. This S-shaped profile is consistent with twist–stretch coupling, in which torsional deformation is coupled to extension, and is well described by a twistable WLC model (blue fit).[33] A schematic representation shows a helical spring wrapped around a cylinder (red), together with a thinner and elongated cylinder (blue), illustrating the twist–stretch coupling mechanism: upon stretching, the helical structure extends while simultaneously reducing its diameter.

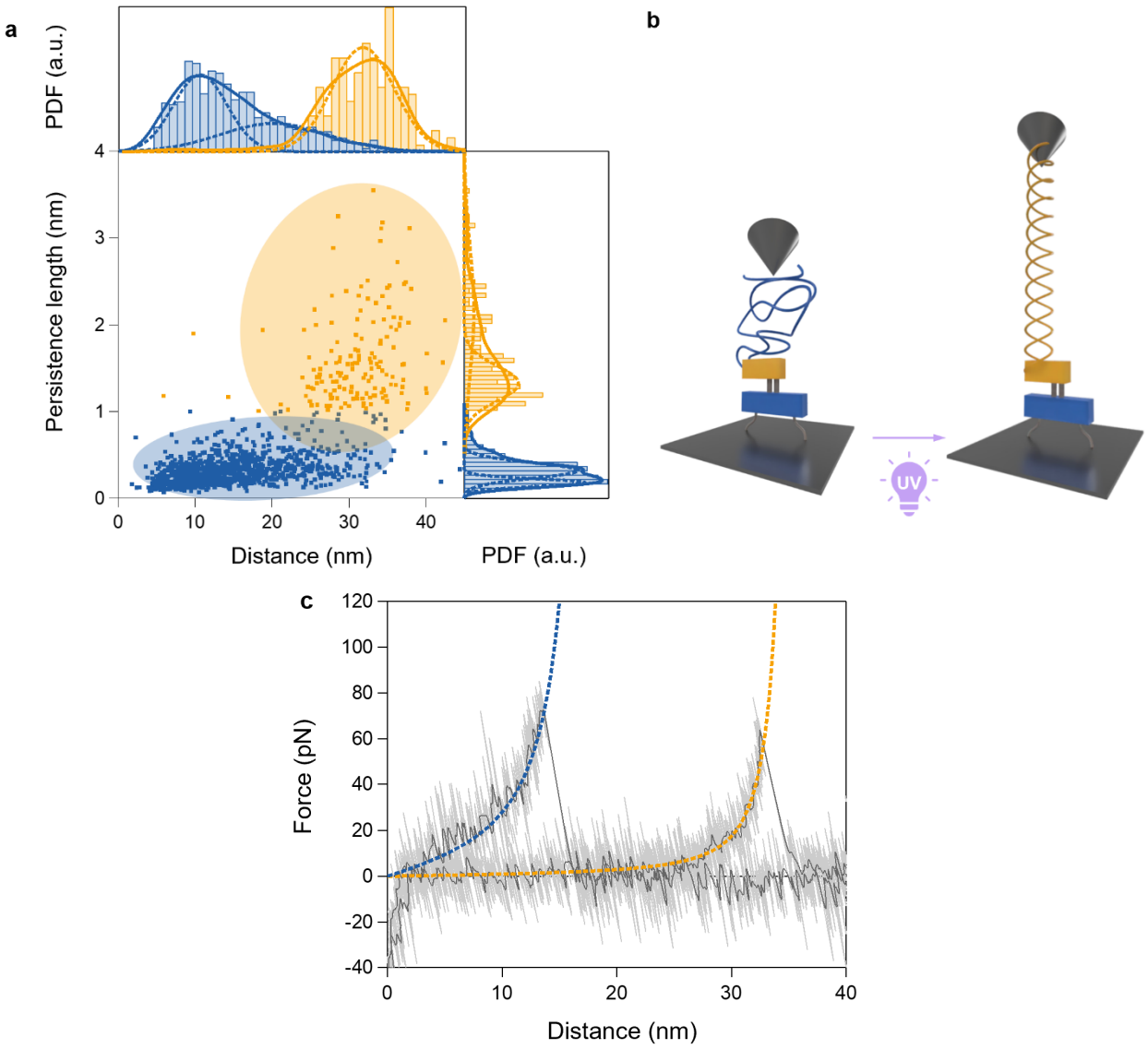

370 **Figure 5. Increased rigidity and extension arising from motor-induced entanglement. a.** l_p values extracted from force–distance curves recorded after UV irradiation of the polymer–motor conjugate, plotted as a function of rupture distance (central scatter plot). The corresponding histograms are shown above (rupture distance) and on the right (l_p), revealing the distributions along each axis. The blue population corresponds to conjugates displaying mechanical properties
375 similar to those observed prior to irradiation, and is therefore attributed to non-entangled configurations. A clear correlation between higher l_p values and larger rupture distances is observed (in orange). The marginal histograms highlight the emergence of two distinct populations, associated with flexible, weakly entangled chains and more rigid, highly entangled structures. **b.** Schematic representation of the conformational transition of the PEO chains from a

random-coil state to a double-helical structure upon UV-induced motor operation **c.** Representative force–distance curves and corresponding WLC fits (dashed lines), illustrating events with standard persistence length (blue) and enhanced persistence length (orange). The raw and smoothed signals are shown in light and dark grey, respectively

References

1. Kay, E. R., Leigh, D. A. & Zerbetto, F. Synthetic Molecular Motors and Mechanical Machines. *Angewandte Chemie International Edition* **46**, 72–191 (2007).
2. Boyer, P. D. The ATP synthase—a splendid molecular machine. *Annual Review of Biochemistry* **66**, 717–749 (1997).
3. Sobti, M., Ueno, H., Noji, H. & Stewart, A. G. The six steps of the complete F1-ATPase rotary catalytic cycle. *Nature Communications* **12**, (2021).
4. Koumura, N., Zijlstra, R. W. J., van Delden, R. A., Harada, N. & Feringa, B. L. Light-driven monodirectional molecular rotor. *Nature* **401**, 152–155 (1999).
5. Li, Q., Fuks, G., Moulin, E., Maaloum, M., Rawiso, M., Kulic, I., Foy, J. T. & Giuseppone, N. Macroscopic contraction of a gel induced by the integrated motion of light-driven molecular motors. *Nature Nanotechnology* **10**, 161–165 (2015).
6. Foy, J. T., Li, Q., Goujon, A., Colard-Itté, J.-R., Fuks, G., Moulin, E., Schiffmann, O., Dattler, D., Funeriu, D. P. & Giuseppone, N. Dual-light control of nanomachines that integrate motor and modulator subunits. *Nature Nanotechnology* **12**, 540–545 (2017).
7. Gao, C., Vargas Jentzsch, A., Moulin, E. & Giuseppone, N. Light-Driven Molecular Whirligig. *Journal of the American Chemical Society* **144**, 9845–9852 (2022).
8. Bao, Y., Luo, Z. & Cui, S. Environment-dependent single-chain mechanics of synthetic polymers and biomacromolecules by atomic force microscopy-based single-molecule force

spectroscopy and the implications for advanced polymer materials. *Chemical Society Reviews* **49**, 2799–2827 (2020).

9. Cheng, B. & Cui, S. Supramolecular Chemistry and Mechanochemistry of Macromolecules: Recent Advances by Single-Molecule Force Spectroscopy. in *Polymer Mechanochemistry* (ed. Boulatov, R.) 97–134 (Springer International Publishing, Cham, 2015). doi:10.1007/128_2015_628.
10. Li, Q., Scholl, Z. N. & Marszalek, P. E. Nanomechanics of Single Biomacromolecules. in *Handbook of Nanomaterials Properties* (eds Bhushan, B., Luo, D., Schricker, S. R., Sigmund, W. & Zauscher, S.) 1077–1123 (Springer, Berlin, Heidelberg, 2014). doi:10.1007/978-3-642-31107-9_13.
11. Lussis, P., Svaldo-Lanero, T., Bertocco, A., Fustin, C.-A., Leigh, D. A. & Duwez, A.-S. A single synthetic small molecule that generates force against a load. *Nature Nanotechnology* **6**, 553–557 (2011).
12. Sluysmans, D., Devaux, F., Bruns, C. J., Stoddart, J. F. & Duwez, A.-S. Dynamic force spectroscopy of synthetic oligorotaxane foldamers. *Proceedings of the National Academy of Sciences* **115**, 9362–9366 (2018).
13. Sluysmans, D., Hubert, S., Bruns, C. J., Zhu, Z., Stoddart, J. F. & Duwez, A.-S. Synthetic oligorotaxanes exert high forces when folding under mechanical load. *Nature Nanotechnology* **13**, 209–213 (2018).
14. Sluysmans, D., Lussis, P., Fustin, C.-A., Bertocco, A., Leigh, D. A. & Duwez, A.-S. Real-Time Fluctuations in Single-Molecule Rotaxane Experiments Reveal an Intermediate Weak Binding State during Shuttling. *Journal of the American Chemical Society* **143**, 2348–2352 (2021).
15. Li, X., Gisbert, Y., Ledent, M., Sluysmans, S., Rapenne, G., Kammerer, C. & Duwez, A.-S. Probing the free rotary oscillations around a single ruthenium atom in an organometallic complex. *Chem* **12**, 102691 (2026).

16. Sluysmans, D., Willet, N., Thevenot, J., Lecommandoux, S. & Duwez, A.-S. Single-molecule mechanical unfolding experiments reveal a critical length for the formation of α-helices in peptides. *Nanoscale Horizons* **5**, 671–678 (2020).

17. Devaux, F., Li, X., Sluysmans, D., Maurizot, V., Bakalis, E., Zerbetto, F., Huc, I. & Duwez, A.-S. Single-molecule mechanics of synthetic aromatic amide helices: Ultrafast and robust non-dissipative winding. *Chem* **7**, 1333–1346 (2021).

18. Asano, M., Sluysmans, D., Willet, N., Bonduelle, C., Lecommandoux, S. & Duwez, A.-S. Single-molecule force spectroscopy shows that side chain interactions govern the mechanochemical response of polypeptide α-helices and prevent the formation of β-sheets. *RSC Mechanochemistry* **2**, 37–44 (2025).

19. Bustamante, C., Bryant, Z. & Smith, S. B. Ten years of tension: single-molecule DNA mechanics. *Nature* **421**, 423–427 (2003).

20. Ritort, F. Single-molecule experiments in biological physics: methods and applications. *J. Phys.: Condens. Matter* **18**, R531–R583 (2006).

21. Marantan, A. & Mahadevan, L. Mechanics and statistics of the worm-like chain. *American Journal of Physics* **86**, 86–94 (2018).

22. Flory, P. J. & Mark, J. E. The configuration of the polyoxymethylene chain. *Die Makromolekulare Chemie* **75**, 11–21 (1964).

23. Dugdale, T. M., Dagastine, R., Chiovitti, A., Mulvaney, P. & Wetherbee, R. Single Adhesive Nanofibers from a Live Diatom Have the Signature Fingerprint of Modular Proteins. *Biophysical Journal* **89**, 4252–4260 (2005).

24. Sarkar, A., Caamano, S. & Fernandez, J. M. The Mechanical Fingerprint of a Parallel Polyprotein Dimer. *Biophysical Journal* **92**, L36–L38 (2007).

25. Zuo, J. & Li, H. Two-Molecule Force Spectroscopy on Proteins. *ACS Nano* **17**, 7872–7880 (2023).

26. Zheng, Y., Han, M. K. L., Zhao, R., Blass, J., Zhang, J., Zhou, D. W., Colard-Itté, J.-R., Dattler, D., Çolak, A., Hoth, M., García, A. J., Qu, B., Bennewitz, R., Giuseppone, N. & del Campo, A. Optoregulated force application to cellular receptors using molecular motors. *Nature Communications* **12**, 3580 (2021).

27. Wang, H., Shen, B., Song, Y., Lee, M. & Zhang, W. Nanomechanical Properties of a Supramolecular Helix Stabilized by Non-Covalent Interactions. *Macromolecular Rapid Communications* **41**, 2000453 (2020).

28. Cluzel, P., Lebrun, A., Heller, C., Lavery, R., Viovy, J., Chatenay, D. & Caron, F. DNA: An Extensible Molecule. *Science* **271**, 792–794 (1996).

29. Oesterhelt, F., Rief, M. & Gaub, H. E. Single molecule force spectroscopy by AFM indicates helical structure of poly(ethylene-glycol) in water. *New Journal of Physics* **1**, 6–6 (1999).

30. Miyazawa, T., Fukushima, K. & Ideguchi, Y. Molecular Vibrations and Structure of High Polymers. III. Polarized Infrared Spectra, Normal Vibrations, and Helical Conformation of Polyethylene Glycol. *The Journal of Chemical Physics* **37**, 2764–2776 (1962).

31. Gore, J., Bryant, Z., Nöllmann, M., Le, M. U., Cozzarelli, N. R. & Bustamante, C. DNA overwinds when stretched. *Nature* **442**, 836–839 (2006).

32. Marin-Gonzalez, A., Vilhena, J. G., Perez, R. & Moreno-Herrero, F. Understanding the mechanical response of double-stranded DNA and RNA under constant stretching forces using all-atom molecular dynamics. *Proceedings of the National Academy of Sciences* **114**, 7049–7054 (2017).

33. Gross, P., Laurens, N., Oddershede, L. B., Bockelmann, U., Peterman, E. J. G. & Wuite, G. J. L. Quantifying how DNA stretches, melts and changes twist under tension. *Nature Physics* **7**, 731–736 (2011).

34. Schiel, P., Maaloum, M., Moulin, E., Nyrkova, I., Semenov, A., Dattler, D., Accou, L.-A., Christoulaki, A., Buhler, E., Plamont, R., Lehn, J.-M. & Giuseppone, N. Supramolecular

polymerization through rotation of light-driven molecular motors. *Nat. Nanotechnol.* **20**, 1052–1061 (2025).